



## Hydration Properties of Cement Pastes with Al-Zinc Oxide and Zinc Oxide Nanoparticles

SeyedAli Ghahari,<sup>1</sup> Ehsan Ghafari,<sup>1</sup> Pengkun Hou<sup>4</sup> and Na Lu<sup>1,2,3\*</sup>

The current study aims to evaluate the influence of aluminum ZnO (AZO) alloys and undoped zinc oxide (ZnO) nanoparticles on hydration behavior of cement paste composites. The study indicated that the addition of AZO nanoparticles resulted in a decrease in the induction period time compared to the addition of ZnO nanoparticles. The effect can be attributed to the aluminum acceleration shields effect, since AZO nanoparticles contain four and five fold coordinated aluminum sites and each of Al site coordinated to six oxygen atoms, the pastes containing AZO exhibited more hydration.

**Keywords:** ZnO nanoparticles; Cement Composite Materials; Hydration behavior

**Received** 11 July 2018, **Accepted** 29 November 2018

**DOI:** 10.30919/esmm5f172

### 1. Introduction

Using nanomaterials for civil infrastructure applications has rapidly increased in recent years.<sup>1-8</sup> Nanoparticles can improve the mechanical properties and durability of cement and concrete composites. By using particles that are smaller than cement particles, denser particle packing and consolidation would be attainable;<sup>9-14</sup> ZnO is one of the most common nanoparticles used as cement additives due to its unique properties including self-cleaning and pollution remediation,<sup>15,16</sup> UV-blocking characteristics,<sup>17,18</sup> gas sensing,<sup>19</sup> and energy harvesting<sup>20</sup> for structures and environment. Furthermore, ZnO has piezoelectric characteristic as it is in a non-centrosymmetric crystallographic phase,<sup>21,22</sup> therefore, it is a promising technology to be used in structural health monitoring applications.

One of the key issues of using ZnO in cement and concrete is its influences on the hydration properties. In cement and concrete industry, ZnO has been used as admixture for cement paste and concrete mixture to tailor intrinsic properties of the composite by taking advantage of its superfine particle size feature, however, retardation on cement hydration is one of the major drawbacks of using ZnO in cement and concrete, especially when setting time should not be elongated.<sup>23,29-31</sup> Study performed by Puertas *et al.* investigated the hydration and leaching behavior of cement mixed with ZnO. It was shown that adding ZnO to the cement paste could significantly prolong the initial and final setting times.<sup>25</sup> Researchers have also studied the effect of zinc ions on the hydration properties of cement paste with supplementary cementitious materials (SCM).<sup>26,27</sup> It showed that the chemical retardation effect of Zn

(II) could be eliminated in metakaolin-cement mixtures, and the modification of the physicochemical property of metakaolin during calcination could be the reason, which resulted in the acceleration of the mixture.<sup>28</sup>

The modification of the physicochemical property of the SCM sheds lights on the potential possibility of using physicochemical-modified Zn to tune the hydration properties of cement. In this study, we have investigated the effect of binary alloys of ZnO nanoparticles additives on hydration behavior of cement paste. This study was designed to systematically investigate the hydration process of cement mixtures reinforced with ZnO and aluminum ZnO alloys (AZO) nanoparticles and their related physical and chemical properties. Samples with 0.2, 0.4, 0.6, 0.8, 1 wt.% ZnO and AZO nanoparticles were prepared and the effect of chemical properties on the hydration behavior of the pastes was examined. X-ray diffractometry (XRD), differential scanning calorimetry (DSC), thermogravimetry analysis (TGA), and fourier-transform infrared (FTIR) spectrometry were performed on the samples in order to elucidate the chemical aspects of the hydration properties. As such, the result of this study can enhance fundamental understanding of ZnO and AZO on hydration behavior of cement.

### 2. Experimental section

All specimens were cast with a Twister Evolution vacuum mixer, and cured with potable water and Portland cement (C) type I 42.5R according to ASTM C150.<sup>32</sup> For maintaining a comparable workability, a polycarboxylate ether based superplasticizer (SP) with a density of 1.108 g/cm<sup>3</sup> was used. As admixture, dry ZnO and aluminum ZnO alloys (AZO) were added to the mixture. The physical and chemical characteristics of cement, ZnO and AZO powders are presented in Table 1 and Table 2, respectively. Table 3 presents eleven series of mixtures, prepared with ZnO, AZO, and a reference mixture without nanoparticles additives. Nanoparticles were incorporated as cement replacement by 0.2, 0.4, 0.6, 0.8, and 1 of weight fractions (wt. %) of cement. The total content of the powder including cement and nanoparticles was kept constant in volume. In addition, the water to binder ratio was kept constant at 0.4 for all the mixtures. At the ages of 3, 7, and 28 days,

<sup>1</sup>Lyles School of Civil Engineering, Sustainable Materials and Renewable Technology (SMART) Lab, Purdue University, USA

<sup>2</sup>School of Materials Engineering, Purdue University, USA

<sup>3</sup>Birck Nanotechnology Center, Purdue University, USA

<sup>4</sup>Shandong Provincial Key Lab for the Preparation and Measurement of Building Materials, Jinan, Shandong, 250022, China

\*E-mail: luna@purdue.edu

**Table 1** Chemical composition and physical properties of cement.

Chemical Analysis	Cement (wt. %)
SiO <sub>2</sub>	20.9
Al <sub>2</sub> O <sub>3</sub>	4.60
Fe <sub>2</sub> O <sub>3</sub>	3.15
CaO	62.0
MgO	2.00
SO <sub>3</sub>	3.60
K <sub>2</sub> O	<1
Na <sub>2</sub> O	<1
Specific gravity	3.14

sample were ground and 100 mesh size powder were mixed with ethanol then heated in a vacuum oven for 24h at 60 °C to stop the hydration process.

In order to study the hydration properties of cement paste, the heat flow rate and cumulative heat release were measured with a TAM Air isothermal calorimeter according to ASTM C1702.<sup>33</sup> The temperature was maintained at 23 ± 0.1 °C during the test. Before starting data acquisition, TAM was set for 30 min to stabilize the baseline. After 10 min from mixing, the cement paste was poured into specific ampoules. The sealed ampoules were then inserted into the TAM chamber and the device started to measure the temperature after reaching the equilibration.

Characterization of phase and crystalline composition were performed by XRD, TGA, and FTIR. The samples were prepared as a power form for XRD analysis with Siemens D500 and thermal gravimetric analysis with TGA Quantachrome Q50. The powder was situated in Cu  $\alpha$  radiation and Ni filter with 50 kV and 30 mA working condition for 4–75° (2 $\theta$ ) range analyzing with step size of 0.02°. Jade software was used for analyzing the results. DSC was performed with TA Instruments DSC 2010 to approve the accuracy of TGA results. Samples were tested in titanium cylinder under a nitrogen gas with a scanning rate of 10 °C/min from 25 °C to 1000 °C. FTIR with Thermo Nicolet Nexus FTIR was used with the ability of quantifying the chemical compositions in the range of 4000-800 cm<sup>-1</sup>. Ten times scan with a resolution of 2.5 cm<sup>-1</sup> was performed during the FTIR analysis. The phase characterization was performed using OMNIC software. In

**Table 2** Properties of ZnO nanoparticles.

Formula	Aluminum content	Specific Surface area (m <sup>2</sup> /g)	Purity	Crystal Phase	Mean Diameter(nm)	Density (g/cm <sup>3</sup> )
ZnO	0	54±20	>99.9 (wt. %)	Zincite (hexagonal)	20±5	5.6
AZO	0.2 (wt. %)	54±20	>99.9 (wt. %)	Zincite (hexagonal)	20±5	5.6

**Table 3** Composition of pastes mixture (by weight, g/cm<sup>3</sup>).

		Cement	Water	SP	ZnO	AZO
Ref	PC	593.9	207.9	2.4	0	0
	ZnO_0.2	592.7	207.9	2.4	1.18	0
ZnO Mixtures	ZnO_0.4	591.5	207.9	2.4	2.37	0
	ZnO_0.6	590.3	207.9	2.4	3.56	0
	ZnO_0.8	589.1	207.9	2.4	4.75	0
	ZnO_1	587.9	207.9	2.4	5.93	0
AZO Mixtures	AZO_0.2	592.7	207.9	2.4	0	1.18
	AZO_0.4	591.5	207.9	2.4	0	2.37
	AZO_0.6	590.3	207.9	2.4	0	3.56
	AZO_0.8	589.1	207.9	2.4	0	4.75
	AZO_1	587.9	207.9	2.4	0	5.93

order to stop the hydration reactions, the samples were stored in acetone bottle for 24h before dried in 60 °C oven.

### 3. Results and discussions

#### 3.1 Hydration analysis

The rate of heat evolution, normalized by the mass of cementitious material (cement and ZnO nanoparticles), as a function of time for paste mixtures containing different dosage of ZnO is shown in Fig. 1. As shown, the addition of ZnO and AZO to the reference sample led to a significant delay in the induction period. The analyzed data including the maximum peak, time to maximum peak, and induction period are presented in Table 4. The samples with elongated induction stage had a delay reaching to hydration peak, leading to a significant lower

cumulative heat. The results indicated that the addition of 1 wt.% ZnO and AZO delayed the hydration up to 110 h and 108 h, respectively. The retardation effect can be attributed to the delay in the formation of C-S-H on the surface of  $C_3S$  in hydration reaction.<sup>34-38</sup> Zinc hydroxide is the product of the reaction between ZnO and water, which has been proven to provide a circumference around the calcium silicate hydrate (C-S-H) layer so that the  $C_3S$  and  $C_2S$  hydration were retarded.<sup>34, 37</sup> Although the  $Zn(OH)_2$  and  $CaZn_2(OH)_6 \cdot 2H_2O$  cannot be detected by XRD, the corroboration of the existence of  $Zn(OH)_3^-$ ,  $Zn(OH)_4^{2-}$  and/or  $CaZn_2(OH)_6 \cdot 2H_2O$  was confirmed by FTIR technique which is discussed further in this manuscript.

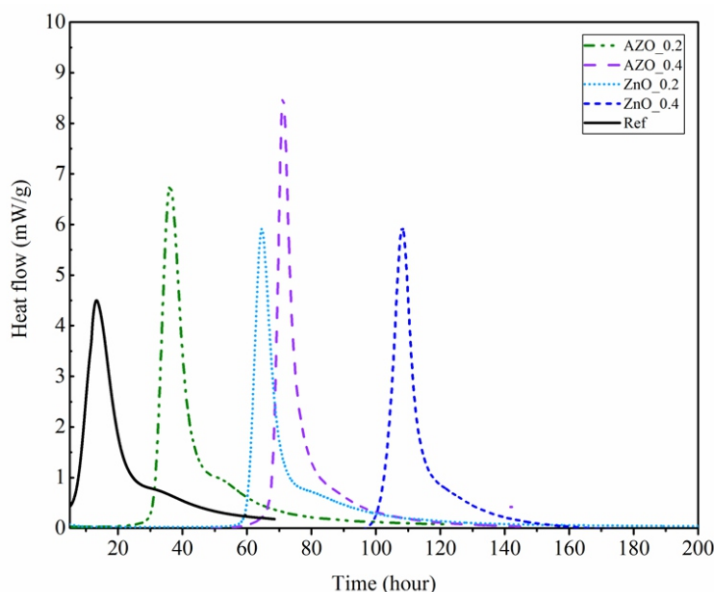
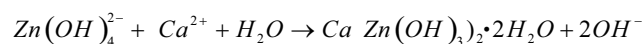


Fig. 1 Heat flow of cement paste containing AZO and ZnO.

Table 4 The obtained hydration parameters from isothermal calorimetry.

Sample		End of induction period (hour)	Time to maximum exothermic peak (hour)
Ref	PC	5	13.3
	ZnO_0.2	58	64.5
ZnO	ZnO_0.4	98	108.3
	ZnO_0.6	98	110.1
	ZnO_0.8	100	104.1
	ZnO_1	102	110.61
AZO	AZO_0.2	25	36.2
	AZO_0.4	60	71.2
	AZO_0.6	82	96.2
	AZO_0.8	94	106.2
	AZO_1	92	108.3

Moreover, the results indicated that the induction period can be reduced significantly by adding AZO\_0.2 and AZO\_0.4 as compared to ZnO\_0.2 and ZnO\_0.4 mixtures. As presented in Table 4, AZO\_0.2 and AZO\_0.4 pastes exhibited roughly a 36 h and 51 h delay in the retardation time to reach the peak comparing to the reference, which is 43 % and 35 % lower than the retardation period of ZnO\_0.2 and ZnO\_0.4 samples. This implies that the higher Al alloy content of AlZnO would lead to a significant change in the early hydration of cement particles and eliminate the retardation effect of ZnO.

### 3.2 XRD

Calcium silicate hydrate (C-S-H), calcium hydroxide (CH), and ettringite phase change and transformation analysis were performed on all mixtures at the ages of 3 and 28 days. The results of XRD analysis are presented in Fig. 2 and Fig. 3. AZO\_1 showed a significant amount of unhydrated cement particles at the age of 3 days. Strong change in peak intensities can be seen between PC and ZnO and AZO. As Fig. 2 shows at 3 days hkl 001 and 012 (CH) is mostly noticeable for PC at 18.5° (2θ). However, for ZnO\_1 and AZO\_1, no significant amount of CH was recognized. This is an indication of delay in hydration at high dosage of ZnO and AZO nanoparticles. Main products of hydration of C<sub>3</sub>S and C<sub>2</sub>S are C-S-H and calcium hydroxide (Ca(OH)<sub>2</sub>) which are produced according to the following exothermic reactions:



ZnO\_0.4 and AZO\_0.4 both had a similar amount of CH at 3 days, slightly lower than that of the Portland Cement (PC). PC had significant lower amount of C<sub>3</sub>S (hkl 204 and 009) and C<sub>2</sub>S (hkl 116, 020) comparing to samples with ZnO or AZO.

Compared to the results obtained at 3 days, XRD analysis for the specimens at 28 days showed a higher amount of calcium hydroxide (CH) for PC, ZnO\_0.4, and AZO\_0.4. The selected results are presented

in Fig. 3. At 18.5° and 34° (2θ) a considerable decrease in the peaks that are related to the less availability of C<sub>2</sub>S and C<sub>3</sub>S, and a comparative increase in the peaks of CH is observable. However, ZnO\_1 and AZO\_1 still show a significant amount of un-hydrated cement, i.e. high amount of C<sub>3</sub>S and C<sub>2</sub>S. The peak of hkl 001 (CH) for ZnO\_0.4 was comparatively lower than that of AZO\_0.4. It was observed that the amount of C<sub>2</sub>S and C<sub>3</sub>S for ZnO\_0.4 were higher than that of the amount of C<sub>2</sub>S and C<sub>3</sub>S for AZO\_0.4. The amount of C<sub>3</sub>S (hkl 204 and 009) and C<sub>2</sub>S (hkl 116, 020) was lower for PC compared to that of ZnO\_1 and AZO\_1. The results imply that the higher Al alloy content in ZnO would change the hydration of cement particles. AZO\_0.2 and AZO\_0.4 showed higher amount of CH at the age of 28 days compared to that of ZnO\_0.2 and ZnO\_0.4, respectively.

### 3.3 DSC/TGA

The evaporation of chemical groups in different mixtures were determined by DSC and TGA using TA Instruments DSC 2010 and Quantachrome Q50, respectively. Fig. 4 and 5 shows the TGA curve and heat flow curve for ZnO\_0.4 and AZO\_0.4 at the age of 28 days, respectively. The results indicated the phase change in the following order: At 105 °C the mass loss is related to evaporable water, followed by an endothermic peak related to the thermogravimetric mass loss at 400-600 °C. This step is associated with the decomposition of the available structural groups. And finally, an exothermic peak regarding the regeneration of new structural groups at 800-1000 °C is available. With higher amount of ZnO and AZO, the endothermic peak area decreased. Subsequently, the peak of the endothermic curve happened at higher temperature. The peak area, presented in Table 5, was calculated with TA Instrument Universal Analysis 2000 software over a standard time range. A linear baseline was implemented for the calculations. No significant change was noticed between the reference sample and the samples containing ZnO\_0.2 and AZO\_0.4 at 28 days, which indicates the fact that at lower dosages, such as ZnO\_0.2 and AZO\_0.4 nanoparticles could interchangeably be used in the cement mixture in a long run.

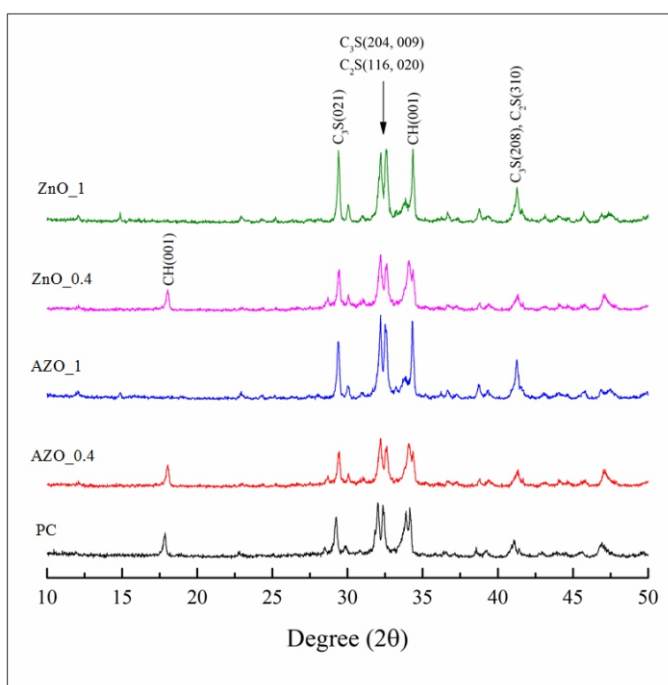


Fig. 2 XRD analysis of paste mixtures containing ZnO and AZO at 3 days.

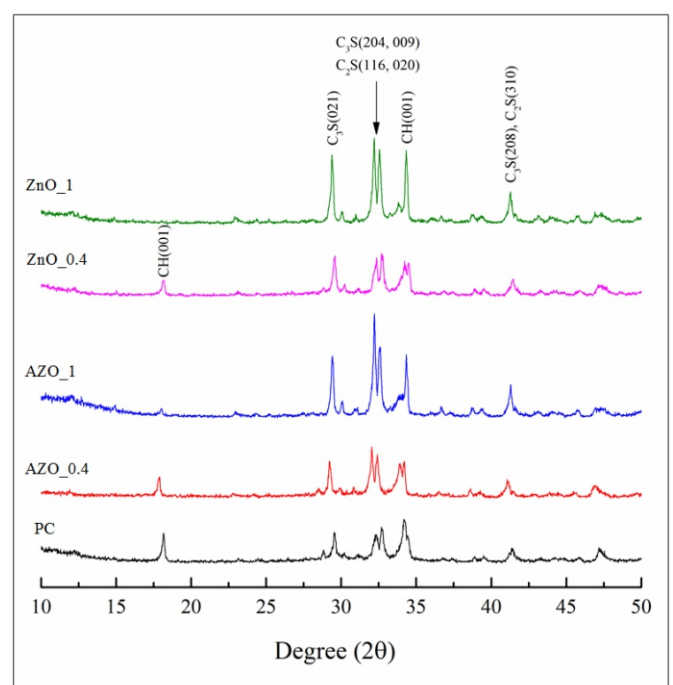


Fig. 3 XRD analysis of paste mixtures containing ZnO and AZO at 28 days.

Mass loss of water is attributed to the cement hydration reactions. The mass losses of cement paste for all specimens were obtained by thermal gravimetric analysis and the corresponding degree of hydration is presented in Fig. 6.

Mass loss of water due to humidity and dehydration of the hydration products during heating, is the first level which happens at 30-350 °C. From the DSC analysis, at 190 °C, Zn(OH)<sub>2</sub> is dehydrated along with other hydration products. The second level of mass loss is attributed to dehydroxylation of CH products. This level happens at 350-530 °C. The next level of mass loss is associated with the decarbonation of calcium carbonate at 530-750 °C, and other products

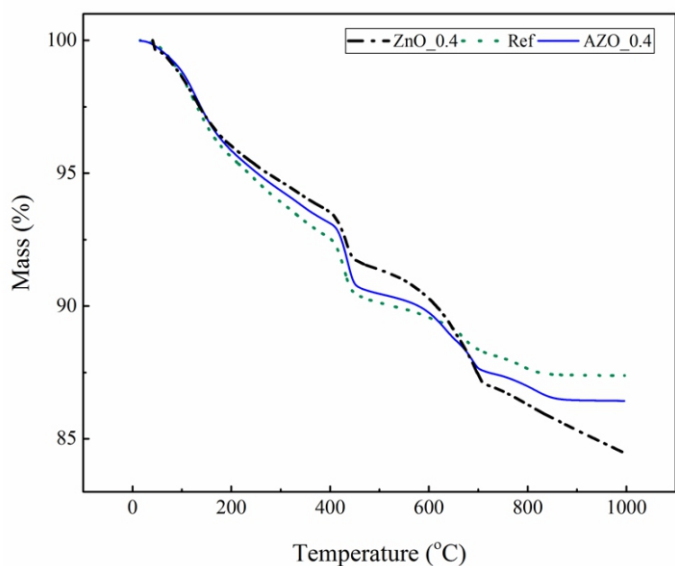
can be categorized at 750-1000 °C. Rough estimation of DOH can be obtained by calculating the difference between the upper part of the TGA curve and the bottom part. ZnO mixes showed a decrease in the amount of the mass loss comparing to the control sample. High amount of ZnO nanoparticles, instead, increased the overall mass loss from 9.83 % to 11.65 %. This value for AZO samples was calculated 14 to 17% higher than that of the ZnO samples, meaning the latter retards cement hydration comparing to AZO. This can be attributed to the nucleation and growth poisoning of C-S-H caused by ZnO nanoparticles detailed as follows.<sup>29</sup> The molecular structure of cement particles and hexagonal wurtzite structure of ZnO nanoparticles are illustrated in Fig. 7. As

**Table 5** Samples endothermic peak (W/g) and related Area (J/g).

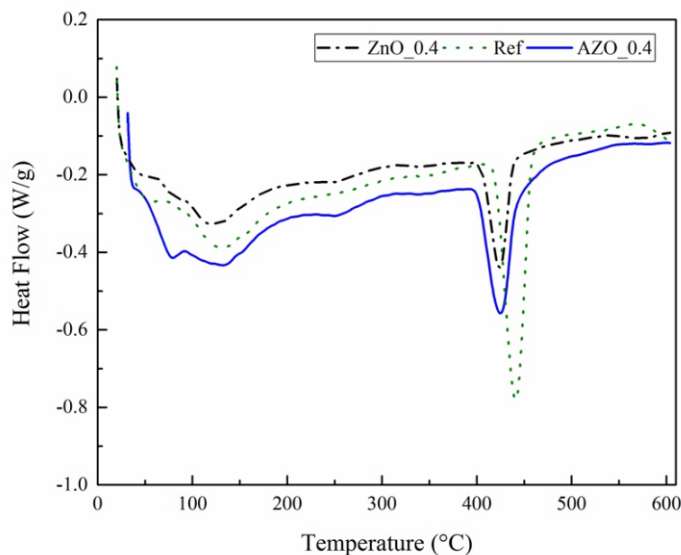
7 days											
Mixture											
DSC	AZO wt. %					ZnO wt. %					
	PC	0.2	0.4	0.6	0.8	1	0.2	0.4	0.6	0.8	1
Endothermic peak (W/g)	-0.70	-0.68	-0.55	-0.51	-0.47	-0.13	-0.58	-0.30	-0.27	-0.16	-0.12
Area (J/g)	14.55	11.27	8.60	7.36	6.05	0.29	11.24	7.59	7.31	0.35	0.09

28 days											
Mixture											
DSC	AZO wt. %					ZnO wt. %					
	PC	0.2	0.4	0.6	0.8	1	0.2	0.4	0.6	0.8	1
Endothermic peak (W/g)	-0.79	-0.73	-0.59	-0.55	-0.52	-0.18	-0.59	-0.42	-0.31	-0.25	-0.16
Area (J/g)	17.11	14.75	10.37	9.02	8.72	0.41	9.31	8.81	7.80	1.08	0.12



**Fig. 4** TGA for 0.4 wt. % ZnO and AZO at the age of 28 days.



**Fig. 5** DSC for 0.4 wt. % ZnO and AZO at the age of 28 days.

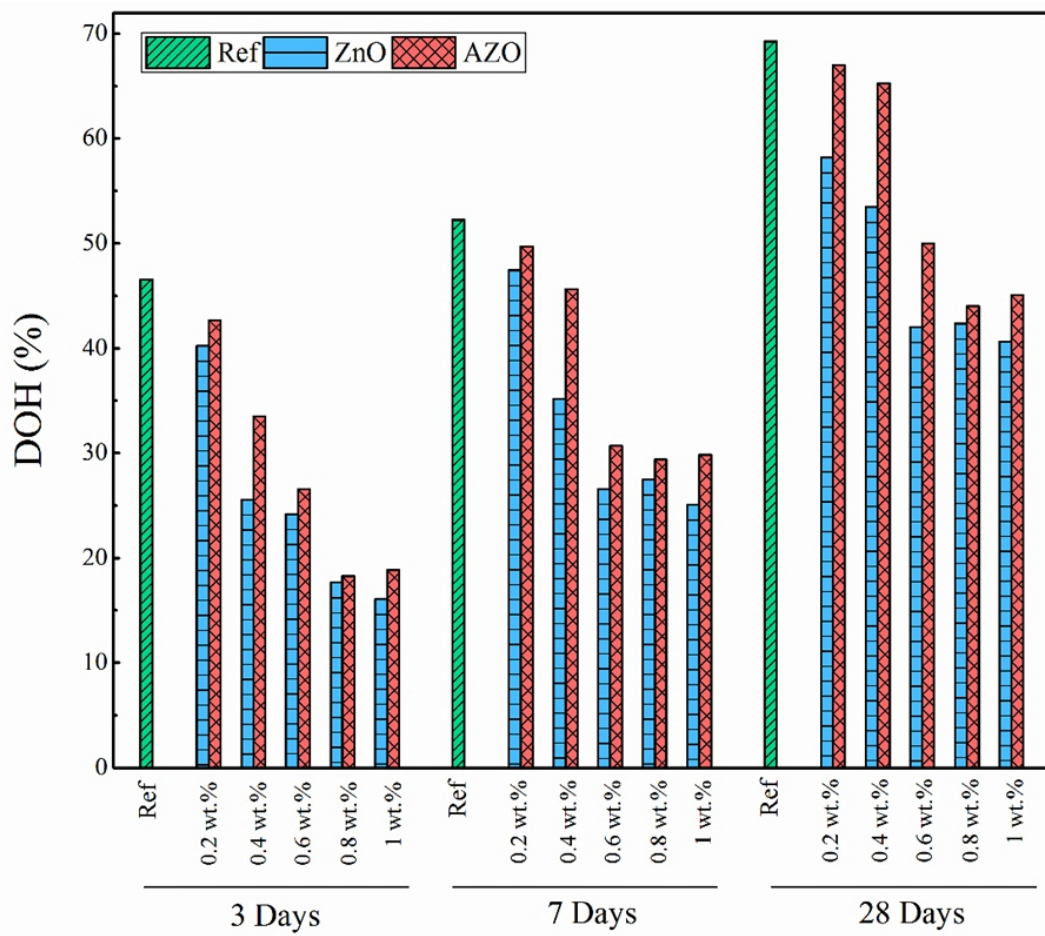


Fig. 6 Degree of hydration for all specimens.

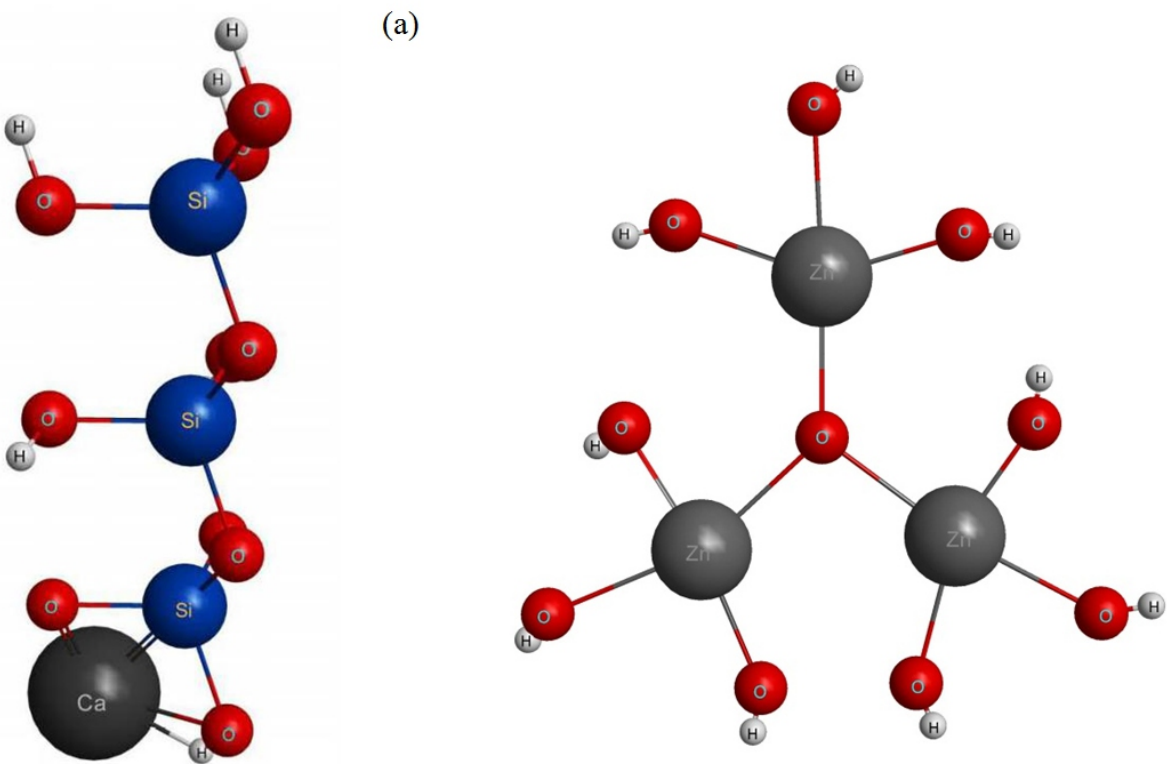


Fig. 7 Molecule structure of cement particle (a) and hexagonal wurtzite structure of ZnO nanoparticle (b)

shown, ZnO has a wurtzite (B4) crystal structure – hexagonal cell with two lattice parameters which forms closed packed (hcp) sublattices. ZnO has tetrahedral coordination and it illustrates sp<sup>3</sup> covalent-bonding.<sup>39</sup> Zn-O has bond dissociation energy of 284.1 kJ/mol and this value for Si-O is 798 kJ/mol. When exposed to C-S-H, ZnO nanoparticles' covalent-bonding are weakened due to the higher attraction forces from silicon and calcium chain molecules. Therefore, it can provide higher number of locations for nucleation sites for cement particles. According to a recent study performed by Avadhut *et al.*, four and five-fold coordinated aluminum sites and an Al site coordinated to six oxygen atoms surround ZnO nanoparticles. Non-conductive phases that are

heavily disordered are available around ZnO nanoparticles.<sup>40</sup>

It is reported that aluminum accelerates the hydration process of cement composite by densification of the interfacial transition zone (ITZ) which leads to the formation of larger crystal of portlandite.<sup>41-43</sup> While no portlandite consumption is reported, C-S-H gel and Ca(OH)<sub>2</sub> have been proven to be formed in the presence of alumina. When AZO nanoparticles are mixed with cement particles, aluminum will first react with the cement particles, and then ZnO nanoparticles will prohibit the hydration to occur. Therefore, adding Al to ZnO can act as an acceleration shields and could improve the hydration properties as expected. DSC data is in agreement with the calorimetry experiment

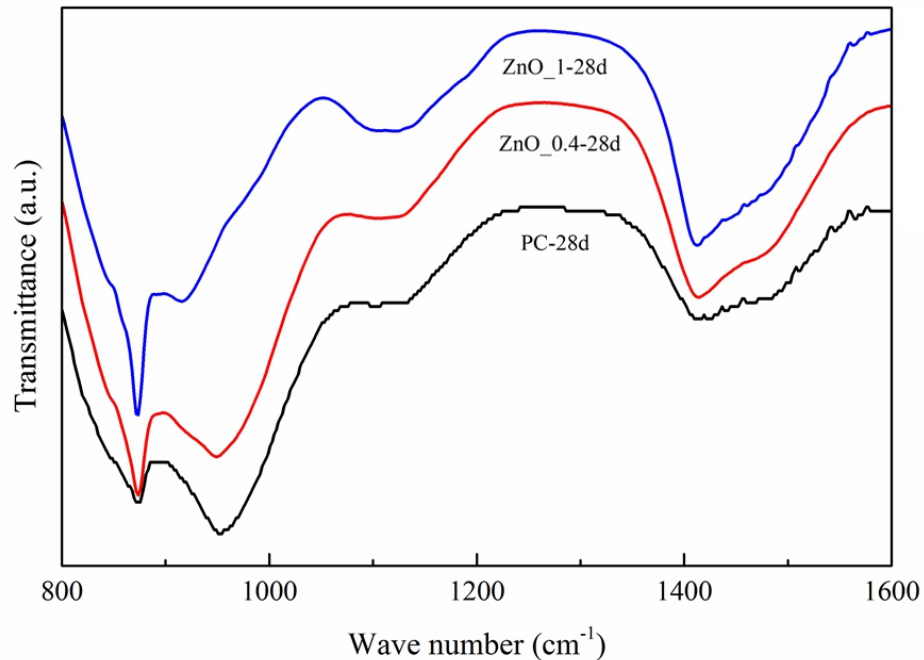


Fig. 8 FTIR spectra for ZnO samples at 28 days ranges from 1600-800 cm<sup>-1</sup>

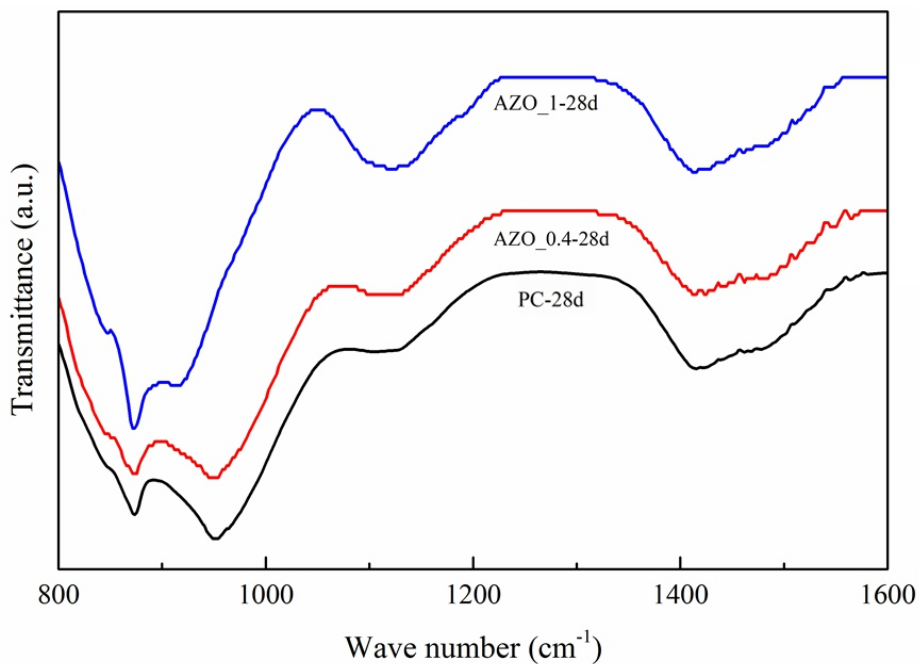


Fig. 9 FTIR spectra for AZO samples at 28 days ranges from 1600-800 cm<sup>-1</sup>

analysis. The degree of hydration (DOH) of PC was increased 5 % with age. Both ZnO and AZO mixes showed a decrease in the amount of DOH while increasing the dosage. The decrease amount is significant at the age of 3 and 7 days. At the age of 28 days, AZO\_0.2 and AZO\_0.4 showed a slight decrease in the amount of DOH compared with PC, i.e. 6 % and 10 % lower than that of the PC mix, respectively. Due to the fact that AZO nanoparticles have the highest surface area to volume ratio among the common concrete particles, it is preferred to use such nanoparticles in the mixture. They can be considered as filler which then makes ITZ and the microstructure denser.

### 3.4 FTIR analysis

Molecular absorption and transmission can be observed by means of FTIR spectra. The molecular finger prints and IR spectral bands for ZnO and AZO are presented in Fig. 8 and Fig. 9, respectively. In some parts of the analysis, possible FTIR peaks from Ylmen *et al.* were used to match our obtained wave numbers.<sup>44</sup> For CO<sub>3</sub>, the related wave number is 1414 cm<sup>-1</sup>, ν<sub>3</sub> for SO<sub>4</sub> is 1109 cm<sup>-1</sup>, and ν<sub>2</sub> for CO<sub>3</sub> is 872 cm<sup>-1</sup>.<sup>41</sup> In general, the dominant band is 920 cm<sup>-1</sup>, which is attributed to asymmetric Si-O stretching (ν<sub>3</sub>) out-of-plane Si-O bending (ν<sub>4</sub>) and in-plane Si-O bending (ν<sub>2</sub>). From 1105 cm<sup>-1</sup>, the SO<sub>4</sub><sup>2-</sup> stretching vibration (ν<sub>3</sub>) can be observed.<sup>36</sup> Also at 1600 cm<sup>-1</sup> wide bands of vibration are available. This could be due to the O-H vibration of water molecules.<sup>45</sup> From 1470-1410 cm<sup>-1</sup>, asymmetric stretching vibration was observed as an indication of CO<sub>3</sub><sup>2-</sup>. At 860 cm<sup>-1</sup> weak bands of CO<sub>3</sub><sup>2-</sup> bending vibration was developed. At 960 cm<sup>-1</sup>, a considerable high frequency band, xCaO · ySiO<sub>2</sub> · 2H<sub>2</sub>O is formed. In the range of 1100-1140 cm<sup>-1</sup> where sulfate is available, a shift to a weaker band (1114 cm<sup>-1</sup>) was observed.

Zn(OH)<sub>2</sub> is an amorphous compound, therefore, it cannot be determined by XRD analysis. According to the FTIR spectra of AZO\_1 wt. %, at the age of 28 days, S-O stretching band has been moved from 1120 cm<sup>-1</sup> to 1102 cm<sup>-1</sup>. Mollah *et al.*,<sup>34</sup> on the other hand, specified that the CaZn<sub>2</sub>(OH)<sub>6</sub> · 2H<sub>2</sub>O is considerably lower than that of CH in terms of quantity, therefore, in XRD analysis it cannot be observed. It is widely known that Zn(OH)<sub>2</sub> are found in high concentration in the porous water.<sup>45</sup> Such ions will react with Ca<sup>2+</sup> ions and CaZn<sub>2</sub>(OH)<sub>6</sub> · 2H<sub>2</sub>O is formed.<sup>36,46</sup> Mollah and Yousuf<sup>47</sup> realized that Zn(OH)<sub>2</sub> which is an amorphous layer causes retardation by covering clinker particles. This will cause further reaction between Ca<sup>2+</sup> ions and zinc hydroxide which produces CaZn<sub>2</sub>(OH)<sub>6</sub> · 2H<sub>2</sub>O. And after this step, hydration process will initiate. FTIR spectra of PC, AZO\_0.4, and AZO\_1 is presented in Fig. 9. At the age of 28 days, considerable difference between PC FTIR spectra and ZnO FTIR spectra was observed, which shows ZnO retardation effect (Fig. 8). However, AZO showed slightly similar spectra to PC which is in agreement with the previous experiments. This shows the fact that AZO could enhance the hydration properties of the cement past compared to that of the cement paste with ZnO, and the results are in agreement with DSC, TGA, XRD analysis. Therefore, AZO compounds can be used in concrete industry to tailor the hydration process of cement paste.

## 4. Conclusions

In this study, the effect ZnO nanoparticles and AZO alloys on the hydration behavior of cement pastes was studied. Results indicated that AZO nanoparticles can improve the hydration properties of cement paste comparing to that of ZnO. When exposed to C-S-H, AZO nanoparticles' covalent-bonding are weakened due to the higher attraction forces from silicon and calcium chain molecules. Therefore, it can provide higher number of locations for nucleation sites for cement

particles. It was found that the pastes containing AZO exhibited better performance in terms of the hydration behavior due to the aluminum acceleration shields, containing four and five fold coordinated aluminum sites and an Al site coordinated to six oxygen atoms. The addition of AZO nanoparticle was found to be effective in reducing the induction period time compared with ZnO nanoparticle, however, this effect is highly influenced by the amount of AZO in the cement composite in that no distinctive behavior on the time to reach the maximum exothermic peak was observed for samples containing AZO more than 0.4 wt. %. At higher concentration than 0.6 wt. %, both AZO and ZnO nanoparticles led to a significant delay in the hydration process.

XRD and TGA analysis depict the fact that at early ages, ZnO nanoparticles cover cement particles leading to a small amount of hydration products. FTIR analysis approves that ZnO acted as a retarder as a clear formation of Zn(OH)<sub>2</sub> and calcium hydrozincate. Retarding action of Zn\_0.2 led to a reduction in the formation of C-S-H which is lower than that of AZO\_0.2. This shows the fact that AZO could enhance the hydration properties of the cement past compared to that of the cement paste with ZnO.

## Acknowledgements

The authors are grateful to Prof. Jan Olek at Purdue University for providing valuable discussion, and the financial supports from National Science Foundation CAREER program (under Grants of CMMI – 1560834).

## References

1. E. Ghafari, S. Ghahari, Y. Feng, F. Severgnini and N. Lu, *Comp. B: Eng.*, 2016, **105**, 160-166.
2. S. Ghahari, 2016.
3. L. Ahmed Sbia, A. Peyvandi, P. Soroushian, A. M. Balachandra and K. Sobolev, *Cons. and Buil. Mater.*, 2015, **76**, 413-422.
4. A. Peyvandi, L. A. Sbia, P. Soroushian and K. Sobolev, *Cons. and Buil. Mater.*, 2013, **48**, 265-269.
5. F. J. Ulm, *Arab. J. for Sci. and Eng.*, 2012, **37**, 481-488.
6. F. J. Ulm, Poromechanics IV - 4th Biot Conference on Poromechanics, 2009.
7. J. Zhao, L. Wu, C. Zhan, Q. Shao, Z. Guo and L. Zhang, *Polymer*, 2017.
8. C. Cheng, R. Fan, Y. Ren, T. Ding, L. Qian, J. Guo, X. Li, L. An, Y. Lei and Y. Yin, *Nanoscale*, 2017, **9**, 5779-5787.
9. M. Aly, M. S. J. Hashmi, A. G. Olabi, M. Messeiry, E. F. Abadir and A. I. Hussain, *Mater. & Des.*, 2012, **33**, 127-135.
10. L. Senff, D. M. Tobaldi, P. Lemes-Rachadel, J. A. Labrincha and D. Hotza, *Cons. and Buil. Mater.*, 2014, **65**, 191-200.
11. M. h. Zhang and H. Li, *Cons. and Buil. Mater.* 2011, **25**, 608-616.
12. E. Ghafari, M. Arezoumandi, H. Costa and E. Júlio, *Cons. and Buil. Mater.*, 2015, **94**, 181-188.
13. T. Tong, Z. Fan, Q. Liu, S. Wang, S. Tan and Q. Yu, *Cons. and Buil. Mater.*, 2016, **106**, 102-114.
14. M. Heikal, S. Abd El Aleem and W. M. Morsi, *HBRC Journal*, 2013, **9**, 243-255.
15. G. Kenanakis, D. Vernardou and N. Katsarakis, *Appl. Cata. A: General*, 2012, **411-412**, 7-14.
16. S. A. Khayyat, M. Abaker, A. Umar, M. O. Alkattan, N. D. Alharbi and S. Baskoutas, *J. of nanosci. and nanotech.*, 2012, **12**, 8453-8458.
17. N. J. Lowe, *Sunscreens: development: evaluation, and regulatory aspects*, CRC Press, 1996.
18. D. B. Brown, A. E. Peritz, D. L. Mitchell, S. Chiarello, J. Uitto and F. P. Gasparro, *Photochem. and photobio.*, 2000, **72**, 340-344.
19. A. A. Tomchenko, G. P. Harmer, B. T. Marquis and J. W. Allen, *Sens. and Actu. B*, 2003, **93**, 126-134.
20. S. Ghahari, E. Ghafari and N. Lu, *Constr. Buil. Mater.*, 2017, **46**, 755-763.
21. S. Minne, S. Manalis and C. Quate, *App. Phys. Lett.*, 1995, **67**, 3918-3920.
22. Z. Guo, S. Wei, B. Shedd, R. Scaffaro, T. Pereira and H. T. Hahn, *J. Mater.*

- Chem.*, 2007, **17**, 806-813.
23. F. F. Ataie, M. C. G. Juenger, S. C. Taylor-Lange and K. A. Riding, *Cem. and Conc. Res.*, 2015, **72**, 128-136.
24. S. B. Neal and A. C. Michael, *Conc. Inter.* 2013, **35**, 42-46.
25. K. G. Kolovos, S. Barafaka, G. Kakali and S. Tsivilis, *Ceramics- Silikaty*, 2005, **49**, 205-212.
26. C. Tashiro and J. Oba, *Cem. and Conc. Res.*, 1979, **9**, 253-258.
27. F. Puertas, I. García-Díaz, M. Palacios, M. F. Gazulla, M. P. Gómez and M. Orduña, *Cem. and Conc. Comp.*, 2010, **32**, 175-186.
28. M. A. Trezza, *Mater. Res.*, 2007, **10**, 331-334.
29. A. Stumm, K. Garbev, G. Beuchle, L. Black, P. Stemmermann and R. Nüesch, *Cem. and Conc. Res.*, 2005, **35**, 1665-1675.
30. S. C. Taylor-Lange, K. A. Riding and M. C. G. Juenger, *Cem. and Conc. Comp.*, 2012, **34**, 835-847.
31. ASTM C150, 2012.
32. M. Yousuf, A. Mollah, R. K. Vempati, T. C. Lin and D. L. Cocke, *Wast. Mana.*, 1995, **15**, 137-148.
33. M. A. Trezza, *Mater. Res.*, 2007, **10**, 331-334.
34. M. Yousuf, A. Mollah, J. Pargat and D. L. Cocke, *J. Env. Sci. & Heal. Part A*, 1992, **27**, 1503-1519.
35. M. Gawlicki and D. Czamarska, *J. ther. anal.*, **38**, 2157-2161.
36. I. F. Olmo, E. Chacon and A. Irabien, *Cem. and Conc. Res.*, 2001, **31**, 1213-1219.
37. M. Vaseem, A. Umar and Y. B. Hahn, American Scientific Publishers: New York, 2010, vol. 5, pp. 1-36.
38. Y. S. Avadhut, J. Weber, E. Hammarberg, C. Feldmann and J. Schmedt auf der Gunne, *Phys. Chem. Chem. Phys.*, 2012, **14**, 11610-11625.
39. S. Barbhuiya, S. Mukherjee and H. Nikraz, *Cons. and Buil. Mater.*, 2014, **52**, 189-193.
40. N. León, J. Massana, F. Alonso, A. Moragues and E. Sánchez-Espinosa, *Biosys. Eng.*, 2014, **123**, 1-11.
41. M. H. Rafieipour, A. Nazari, M. A. Mohandesi and G. Khalaj, *Mater. Res.*, 2012, **15**, 177-184.
42. R. Ylmén, U. Jäglid, B. M. Steenari and I. Panas, *Cem. and Conc. Res.*, 2009, **39**, 433-439.
43. T. Nochaiya, Y. Sekine, S. Chooapun and A. Chaipanich, *J. Alloys and Comp.*, 2015, **630**, 1-10.
44. M. Gawlicki and D. Czamarska, *J. Therm. Anal. Calor.*, 1992, **38**, 2157-2161.
45. M. Y. A. Mollah, F. Lu and D. L. Cocke, *Sci. Total. Environ.*, 1998, **224**, 57-68.